This project has received funding from the Euratom research and training programme 2014-2018 under grant agreement No 662287.

EJP-CONCERT

European Joint Programme for the Integration of Radiation Protection Research

H2020 – 662287

D9.107 – Prototype of fast MC real time radiation dose estimate application to be tested in hospitals

Lead Author: MA. Duch
With contributions from: A. Almén, M. Andersson, V.G. Balcaza, A. Camp, M. Ginjaume, J. Sempau, A. von Barnekow

Reviewer(s): F Vanhavere
and CONCERT coordination

Work package / Task	**WP9**	**T9.6**	**ST 9.6.2**	**SST9.6.2.3**
Deliverable nature:	**Report**			
Dissemination level: (Confidentiality)	**PU**			
Contractual delivery date:	**2019-12-30 (M55)**			
Actual delivery date:	**2019- 12-23 (M55)**			
Version:	**1**			
Total number of pages:	**26**			
Keywords:	**interventional radiology, MC simulation, feasibility**			
Approved by the coordinator:	**M55**			
Submitted to EC by the coordinator:	**M55**			

CONTENT

I. Introduction

The objective of the PODIUM project is to develop a user-friendly online tool (DCA) to calculate the radiation dose to workers. Dose calculations will be performed based on two inputs: (i) the position of workers (in real time) and (ii) the spatial distribution of the radiation field, including its energy and angular distribution. This information is used to generate the needed input files for the developed dose calculation engines.

It was foreseen to provide fast dose calculations by using two approaches. The first approach would use a library of pre-calculated conversion coefficients, while the second one would be based on the use of fast Monte Carlo (MC) simulations with the MC-GPU code and other accelerated calculations with standard codes such as PENELOPE. The main aim of task 2.3 is to test the speed and resulting accuracy of the latter approach, based on MC codes.

The goal of this report is to present the two fast MC codes developed for interventional radiology:

- MCGPU-IR.
- PENELOPE/penEasyIR.

The report describes the methodology applied in both systems. The MC results are compared with the measurements in D9.110 and, finally, an analysis of calculation speed is presented.

II. Methodology

The two fast Monte Carlo approaches used for the dose calculations read input files adapted by the PODIUM application. The DCA organizes them as it is required by each Monte Carlo code, Figure 1 summarizes the dose calculation workflow and the information required to obtain the occupational dose based on the PODIUM approach.

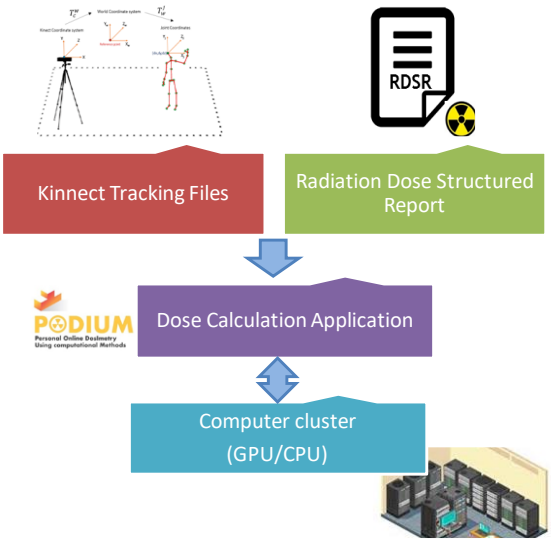

Figure 1. Dose calculation workflow.

In interventional radiology workplaces the scattered radiation field that reaches the medical staff should be calculated with clinic and patient specific data, but for both MC codes the same basic information is needed. The most important data is detailed in the following section.

II.1 Radiation field required information

II.1.1 Required information and data sources

Some of the needed data correspond to the physical configuration of the X-ray tube, this could be considered as fixed values for a specific room and gathered during the setting-up of the dosimetry application in the facility, see D9.106. However there are patient specific data that have to be retrieved in real-time or at least be available at the end of a procedure:

- Sex, height and weight of the patient. This information should be introduced by the operator in the DCA.
- Anatomical region examined-procedure type. If the position of the C-arm and/or the origin of table movements are not well-known, this information would be alternatively used.
- For each projection/irradiation event:
    - Date/time it started, duration. This Information will be needed to determine the position and posture of the monitored worker according to tracking data.
    - Focal spot position.
    - Shape and size of the radiation field.
    - Source to image intensifier distance.
    - Source rotation angles.
    - kVp (kV).
    - Added filtration.
    - Dose at the reference point, for normalization purposes, or the dose area product (DAP).
    - Position of the reference point. Alternative value for normalization purposes if the DAP is not available or inconsistent.
    - Position of movable protective elements (table shields, ceiling-mounted or wall-mounted shields…).
    - Patient's table position (x,y,z) in (cm).

As it was stated in D9.106, for the PODIUM project the preferred source to retrieve this data will be the Radiation Dose Structured Report (RDSR), which is generated at the end of the medical procedure. However, if this information could be obtained in real time, the DCA is structured so that it could be easily adapted to correctly deal with real-time information of the irradiation event (during the procedure).

Radiation source description

For both MC codes the X-ray beam is computationally collimated to produce a rectangular field on the image intensifier plane according to the field size and shape indicated in the RDSR. The image intensifier is automatically located at the specified distance right in front of the source focal spot, with the collimated beam pointing towards the geometric centre of the detector (see Figure 2).

The energy distribution of the X-ray beam is generated according to the X-ray systems characteristics and procedure specific data (anode material and anode angle; inherent and added filtration, kVp). Figure 3 shows the comparison between the beam energy distribution generated by the PODIUM system (based on SPEKTR, Punnoose 2016) and XCOMP5R (Nowotny 1985), which is a well-known code. Differences between the doses calculated by using the PODIUM system or XCOMP5R are lower than 2 %.

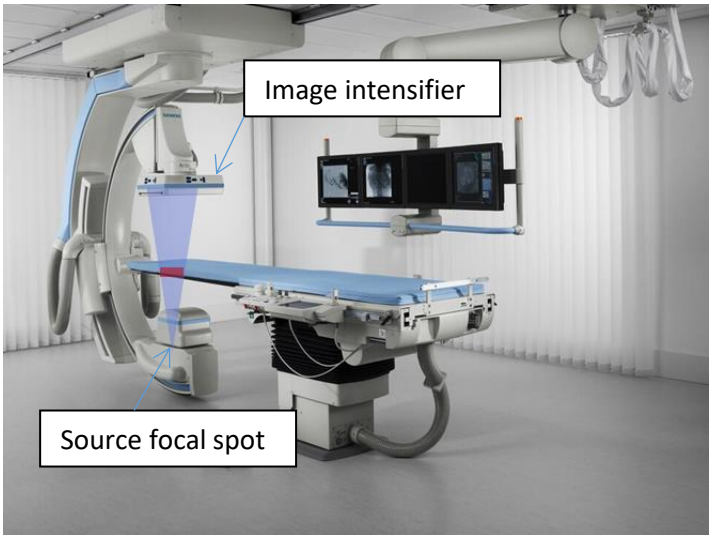

Figure 2: Source description.

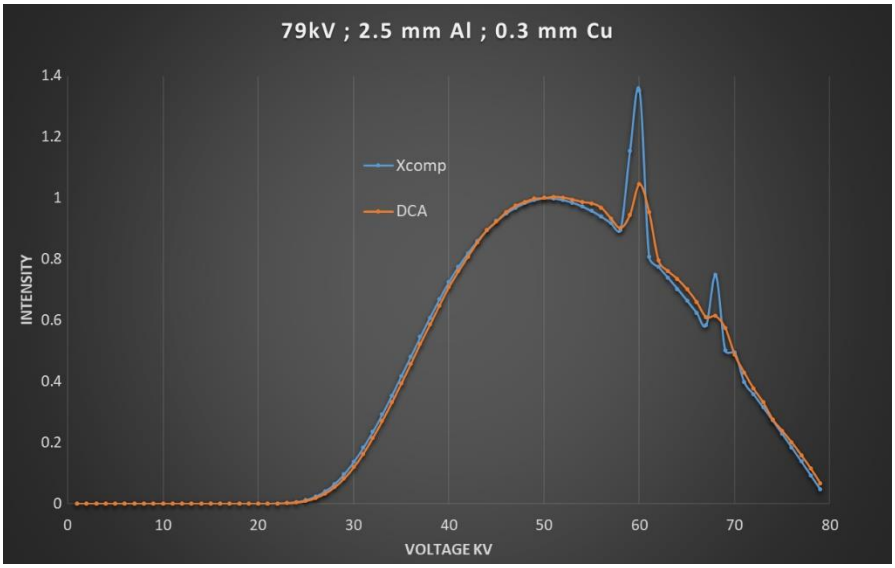

Figure 3: Comparison of the energy distribution of the X-ray beams generated by PODIUM system and XCOMP5R.

II.1.2 Normalization to absolute values

All Monte Carlo codes need a normalization factor *N* to refer the simulated absorbed dose per history to the real number of emitted photons.

$$N = \frac{entrance\ air\ kerma}{K_a} \quad (1)$$

For each irradiation event (fixed kV, filtration, angulation and field size values), *N* is calculated from the ratio between experimental entrance air kerma and simulated air kerma (K_a) or energy deposited at a point of interest. K_a must be calculated in a point where there is no influence of backscatter in order to simulate same conditions as experimental entrance air kerma value.

In general the experimental entrance air kerma at the point of interest will be calculated following the inverse square law from the dose area product (DAP) value divided by the radiation field-size, both values supplied in the RDSR (see equation 2). As an alternative, the dose at the reference point reported in the RDSR can also be used. It is worth mentioning that in the energy range of interventional radiology kerma and absorbed dose are assumed to be equal.

$$entrance\ air\ kerma = \frac{DAP}{field\ size} \cdot \frac{(distance\ source - detector)^2}{(distance\ source - point\ of\ interest)^2} \qquad (2)$$

II.2 PENELOPE/penEasyIR

PENELOPE/penEasyIR is based on PENELOPE v2014 (Salvat 2014), a standard general-purpose MC code. The code performs Monte Carlo simulation of coupled electron-photon transport in arbitrary materials for a wide energy range, from a few hundred eV to about 1 GeV. Photon transport is simulated by means of the standard, detailed simulation scheme.

The code is freely distributed by the OECD Nuclear Energy Agency Data Bank (https://www.oecd-nea.org/databank) and, in North America, by the Radiation Safety Information Computational Center of the Oak Ridge National Laboratory (https://rsicc.ornl.gov). The core of the system is a set of Fortran subroutines that run in central processing units (CPU).

Besides, penEasy (Sempau 2011) is a general-purpose main program for PENELOPE that includes a set of source models, tallies and variance-reduction techniques that are invoked from a structured code. The program has been modified for the specific purposes of PODIUM project in the interventional radiology field, and the new program has been named penEasyIR. As a whole, the system will be called from now on PENELOPE/penEasyIR.

To speed-up the simulation process by using a general purpose MC code such as PENELOPE, two main approaches have been used:

- Use of a variance reduction technique to calculate operator doses. In particular the Detection forcing technique implemented in PENELOPE/penEasyIR as tally 'Photon Fluence Point' (now publicly available in penEasy v20190921 (https://inte.upc.edu/en/downloads).
- Simplification of the geometry of the problem.

Detection forcing technique

The PENELOPE/penEasyIR tally Photon Fluence Point virtually computes the photon fluence spectrum at a detection point specified by its position coordinates. The fluence can be defined as the number of photons per unit area reaching a small test sphere centered at the point of interest. A direct application of this definition to calculate the scattered field that reaches the medical staff in interventional radiology is impractical. A more effective approach is to use a detection forcing technique. The idea underlying the method is that, instead of counting photons that actually reach the test sphere, the probability per unit cross sectional area of reaching the sphere is tallied. Afterwards the linear attenuation coefficient (i.e., inverse mean free path) of the m-th material encountered by the virtual photon along its straight line path towards the point of interest and the distance travelled in that material is taken into account to compute the probability to reach the test sphere.

The fluence produced by the present tally is not equivalent to the one produced with the tally Fluence Track Length, which is fully consistent with PENELOPE's physics. To prevent some statistical fluctuations and non-convergence of the results, an exclusion sphere (1 cm radius) surrounding the detection point has been included.

By using this technique the simulation times are drastically reduced. In a typical interventional radiology procedure where only scattered radiation reaches the medical staff, up to several days would be needed to calculate the absorbed doses at the point of interest with PENELOPE/penEasy without any variance reduction technique applied (statistical uncertainties lower than 1%, k=1). On the contrary, with PENELOPE/penEasyIR the simulation times are reduced to tens of seconds, with similar statistical uncertainties.

Geometry simplications

The simulation speed highly depends on the complexity of the geometrical description of the problem. The simulation of a complex patient description needs calculations six times longer than a simplified phantom to obtain results with a comparable uncertainty. Therefore, to speed-up the simulation process, a simplified humanoid phantom has been selected for the patient anatomical description (see section II.2.1) made of one single material (ICRU tissue) which also provided accurate results, within accepted uncertainties.

Simulation process

PENELOPE/PenEasyIR provides the photon energy fluence distribution at a given position and subsequently fluence to dose conversion coefficients are automatically applied to obtain the operational quantities: $H_p(10)$, $H_p(3)$, $H_p(0.07)$. For additional details see section II.2.2.

The files needed to set up the simulation (through plain text files which are prepared by the DCA) are:

- Main input file that initializes the code and sets the simulation parameters for each irradiation event to be simulated: simulation time, focal spot position, operator position, shape and size of the radiation field, source to image intensifier distance, source rotation angles, normalization values, as described in section II.1.
- Input file containing the photon energy distribution emitted by the X-ray tube, as described in section II.1
- A file with the patient geometry adapted to the actual sex, height and weight of the patient, details about the applied methodology in section II.2.1.
- For each material index listed in the geometry file, the corresponding material file.

Finally, the methodology applied by PENELOPE/penEasyIR for the operator positioning and calculation of the operational quantities is described in section II.2.2.

II.2.1 Patient anatomical description

PENELOPE/PenEasyIR describes the patient by means of quadric surfaces (spheres, cylinders…), in general the selected geometry is a BOMAB-like phantom, see Figure 4, but other geometries can be easily used. The BOttle Mannequin ABsorber (BOMAB) phantom provides a functional simulation for the scattering of radiation in an adult human figure 170 cm tall and is immersed in air.

Table 2: BOMAB characteristics.

	Shape	Cross section (cm)	Vertical height (cm)
Head	Ellipse	19x14	20
Neck	Circle	13 ϕ	10
Thorax	Ellipse	30x20	40
Lumbar	Ellipse	36x20	20
Thighs (2)	Circle	15 ϕ	40
Calves (2)	Circle	12 ϕ	40
Arms (2)	Circle	10 ϕ	60

Phantom scaling

In order to adapt the phantom's dimension to the patient characteristics, the body mass index (BMI) factor defined in equation (3) is applied.

$$BMI = \frac{Weigth\,(kg)}{Heigth(m)^2} \qquad (3)$$

First, the height of the phantom is scaled to adjust exactly to the height of the patient. The two other dimensions (width and depth) are obtained comparing the BMI values with the waist perimeter. Note that we are assuming the phantom waist as a perfect ellipse. Depending on the irradiated part of the body, another organ could be considered for normalization.

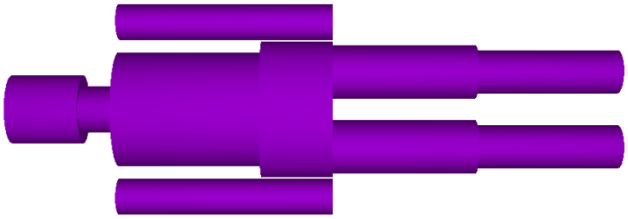

Figure 4: PENELOPE/penEasyIR patient description.

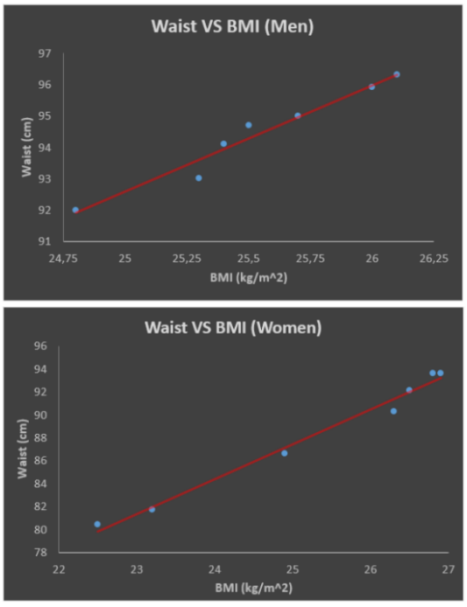

Figure 5: Waist diameter as a function of BMI.

Figure 5 shows the correlation between BMI and waist perimeter for both men and women (data obtained from Wells et al 2007).

The equations for both linear approximations are:

$$waist_{men}(cm) = 3.3602 * BMI_{men}\left(\frac{kg}{m^2}\right) + 8.599 \qquad (4)$$

$$waist_{women}(cm) = 3.0254 * BMI_{women}\left(\frac{kg}{m^2}\right) + 11.787 \qquad (5)$$

II.2.2 Operator positioning and normalization to absolute values

Photon energy fluence is simulated at up to 4 (in a single run) points in air, matching operator Kinect joints (Points B in Figure 6).

The normalization factor mentioned in section II.1.2, equation 1, is calculated at the same time than the operator doses. To do so, the geometry already contains an air box where the air kerma is calculated by using the 'Track fluence length' tally.

$H_p(10)$ received by the operator is calculated applying Equation 6 (ICRP, 1996). Similarly $H_p(0.07)$ and $H_p(3)$ can be calculated with the same equation but using, respectively, $(H_p(0.07,0º)/K_a)$ and $(H_p(3,0º)/K_a)$ from Gualdrini 2013 et al instead of $(H_p(10,0º)/K_a)$.

$$H_p(10)[\mu Sv] = N \cdot F \cdot \sum_{i=1}^{n} \phi_i^{sim} \cdot \left(\frac{\mu_{tr}}{\rho}\right)_i \cdot E_i \cdot \left(\frac{H_p(10,0º)}{K_a}\right)_i \qquad (6)$$

Where

- N is the normalization factor.
- F is a unit normalization factor $1.602 \cdot 10^{-13}$ [J g kg^{-1}]
- ϕ_i^{sim} is the simulated energy fluence, from Tally Photon Fluence Point, for energy region i at point B [cm^{-2} eV^{-1} per history].
- $\left(\frac{\mu_{tr}}{\rho}\right)_i$ is mass energy-transfer coefficient for energy region i [cm^2 g^{-1}] which at those energies is comparable to $\left(\frac{\mu_{en}}{\rho}\right)$ and can be interpolated from NIST.
- E_i is the middle energy for energy region i [eV].
- $\left(\frac{H_p(10,0º)}{K_a}\right)_i$ is the conversion coefficient from air kerma free-in-air to $H_p(10,0º)$ in an ICRU slab for energy region i, interpolated from ICRP74.

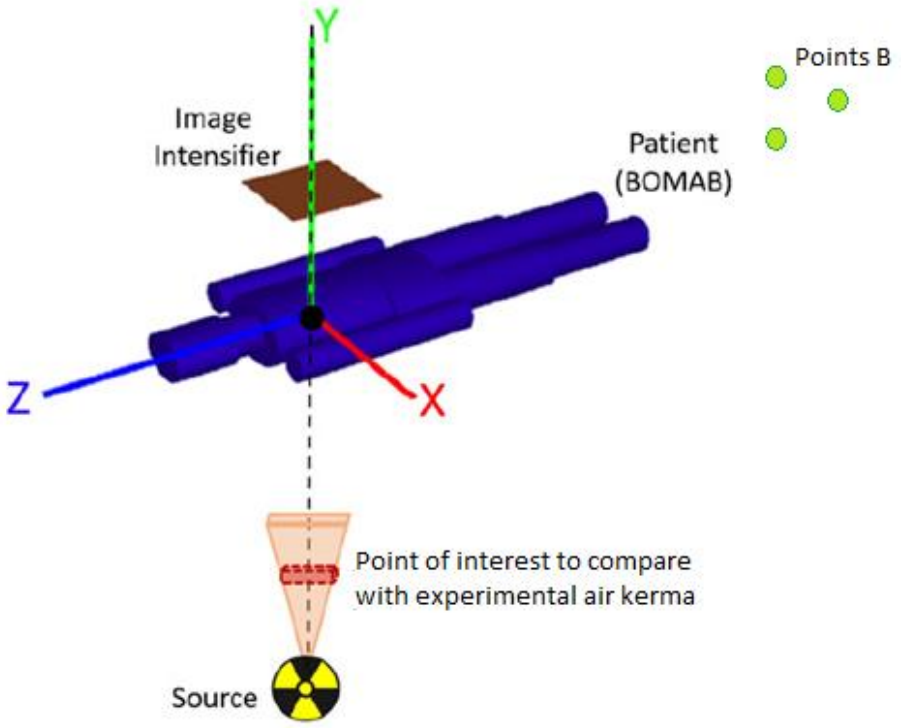

Figure 6: Scheme of geometry used in PENELOPE/penEasyIR simulation.

II.2.3 Simulation of ceiling-mounted shields

PENELOPE/penEasyIR allows the user to define a shield interposed between the main operator and the radiation source by indicating the material composition and dimensions, however to do it automatically the camera system should provide the position and orientation of the shield. At present, when shields are used, the geometry files have to be prepared manually.

II.3 MCGPU-IR

MCGPU-IR is based on MC-GPU (Badal 2009), being the latest version of this software the one released in 2012. MC-GPU is a Monte Carlo simulation code that generates synthetic radiographic images and computed tomography (CT) scans of realistic models of the human anatomy using the computational power of commodity Graphics Processing Unit (GPU) cards. The code implements a massively multi-threaded Monte Carlo simulation algorithm for the transport of X-rays in voxelized geometries. The X-ray interaction models and material properties were adapted from PENELOPE v2006. The interaction sampling and geometry ray-tracing algorithms were designed to provide an optimum performance in GPUs, minimizing the accesses to the slow video memory while maximizing the parts of the code that can be executed in parallel in thousands of concurrent GPU threads.

MC-GPU was developed using the CUDA programming model from NVIDIA to achieve maximum performance on NVIDIA GPUs. The code can also be compiled with a standard C compiler to be executed in a regular CPU; however it has been tested only in the Linux operating system. In a typical medical imaging simulation, the use of GPU computing with MC-GPU has been shown to provide a speed up of between 20 and 40 times, compared to the execution on a single CPU core.

The source code of MC-GPU is free and open software in the public domain, and is distributed from the website: https://code.google.com/archive/p/mcgpu/.

In 2013, A. Badal et al. developed MC-GPU beta, an extension of the original MC-GPU which added some new features, being the most important one the possibility to simulate staff doses (single operator); and afterwards the possibility of simulating shields interposed between the source and the operator. MC-GPU beta is not yet publicly available.

MC-GPU beta has been modified during PODIUM project to speed-up the simulations. The new version allows an automatic simulation of the source parameters, updates physical models, and finally corrects some programming bugs. It is specifically designed for interventional radiology and will be called from now on MCGPU-IR.

To speed-up the simulation process two main approaches have been used:

- Parallelization among several GPU cards by the implementation of MPI libraries.
- A set of functions have been developed to automatically set the optimal values for:
    - Number of blocks per kernel.
    - Number of threads per block.
    - Number of histories per thread to be simulated in the GPU.

The non-optimized code running in one single (GPU) needed longer simulation times (up to a factor of 4) than the optimized code running with two GPU cards.

Simulation process

In MCGPU-IR two simulations are successively launched: a simulation with the patient anatomy to compute the patient average and peak organ doses and 3D dose map, and a separate simulation with the operator anatomy to estimate the operator doses.

As indicated in section II either for PENELOPE/penEasyIR and MCGPU-IR the same basic information is needed, but the input files have a different format and coordinate systems. In particular, the code needs several input files:

- Main input file that initializes the code and sets the simulation parameters for the simulation of the patient; and a secondary input file where the relative position of the X-ray source and the operator is included as well as the shape and size of the radiation field, source to image intensifier distance, source rotation angles for each irradiation event to be simulated.
- A file for each photon energy distribution emitted by the X-ray tube.
- A file with the patient/operator voxelized geometry, listed in the main input file. The voxelized geometry is a box that contains the anthropomorphic phantom surrounded by air. The patient and the operator must be the same phantom but they can be scaled differently to adapt their dimensions to the real dimension of the patient and of the worker.
- For each material index listed in the voxelized geometry, the corresponding material file.

With this information, for each irradiation event, a dosimetric simulation loop is executed to calculate the worker's effective dose and organ doses.

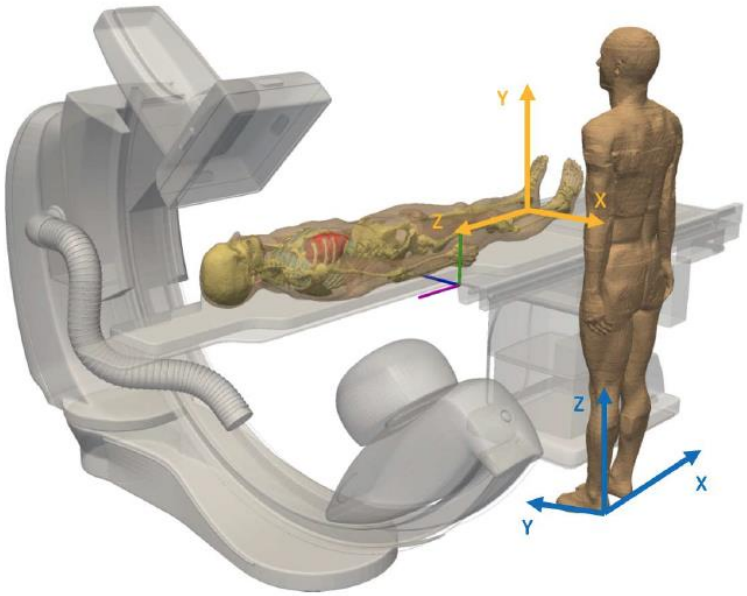

Figure 7: Voxelized phantoms for patient/operator.

During the simulation with the patient anatomy all the particles escaping the simulation universe are tested for intersection with the operator bounding box. Those X-rays scattered in the direction of the operator are stored in a phase space file (PSF) in GPU memory. When the simulation with the patient finishes, a new simulation with the operator anatomy is started using the PSF as the X-ray source. Since only a small fraction of the initial X-rays are expected to be scattered towards the operator, each X-ray in the PSF is recycled many times to maximize the information obtained from each particle as an intrinsic variance reduction technique.

At the end MCGPU-IR provides absorbed dose at a voxel level, the absorbed dose in the different specified organs in the phantom file (if the voxelized phantom is segmented), and finally the effective dose is computed (ICRP, 2007).

II.3.1 Patient/operator anatomical description

During PODIUM, MCGPU-IR used the voxelized Rex or Regina phantoms developed by Helmholtz Zentrum München - HMGU (Figure 8).

The number and dimensions of the considered voxels in each case are:

Table 3: REX characteristics.

Rex	Voxels	Dim vox (cm)	Dim (cm)
X	254	0.2137	54.28
Y	138	0.2137	29.49
Z	222	0.8	177.60

Table 4: REGINA characteristics.

Regina	Voxels	Dim vox (cm)	Dim (cm)
X	299	0.1775	53.07
Y	148	0.1775	26.27
Z	348	0.484	168.43

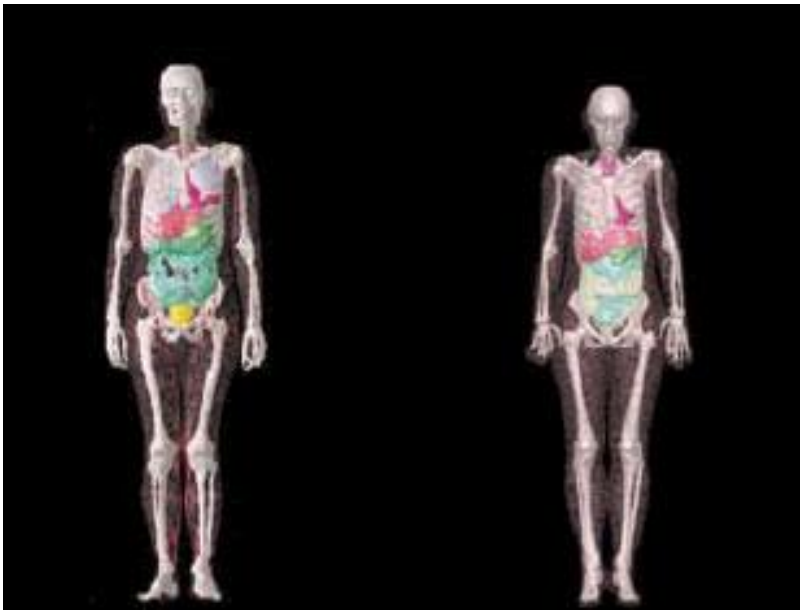

Figure 8: REX and REGINA voxelized phantoms.

For PODIUM, the 143 tissues from the original phantoms were reduced to 26: air surrounding; cortical bone; spongious bone; heart; remaining tissues (soft tissue); front skin trunk; back skin trunk; other skin (extremities); blood; muscle; cartilage; lung; oesophagus; thyroid; bladder; liver; bone marrow; breast adipose; breast glandular; colon; stomach; gonads (ovaries & testes); salivary glands; brain; eye lens left; eye lens right. This organs segmentation allows calculating the effective dose and the dose equivalent of extremities and of the lens of the eye.

$H_p(10)$ is calculated as the mean absorbed dose at eight voxels made of ICRU tissue at a depth of approximately 1 cm, at the position of interest.

As mentioned before, the latest version of MC-GPU was based in the photon interaction models of PENELOPE v2006, however several PENELOPE versions have been released since then. During the PODIUM project the latest version of PENELOPE is PENELOPE v2014. There have been few changes

between the PENELOPE versions of 2006 and 2014, thus, the photon cross-sections were modified (see Figure 9). For MCGPU-IR the material's description has been updated to the newest available interaction models.

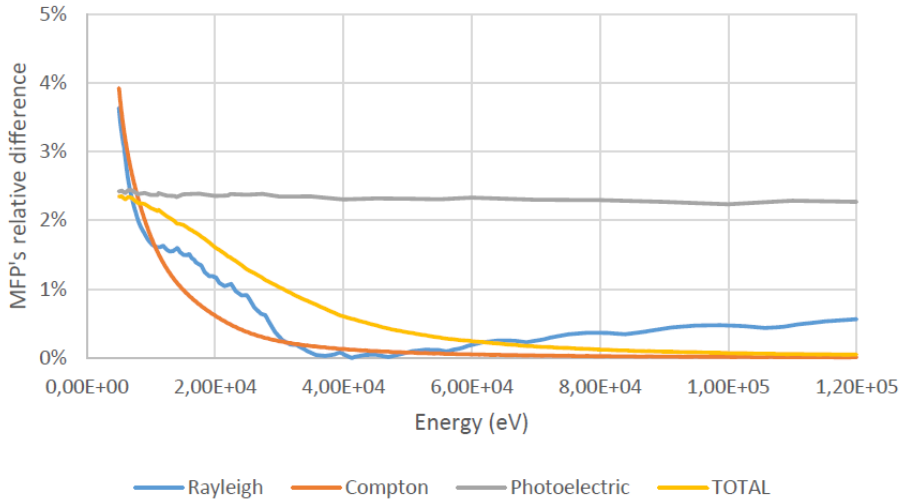

Figure 9: Relative differences between photon mean free paths (MFP) from PENELOPE v2006 and v2014.

Phantom scaling

The phantom scaling methodology is the same than for PENELOPE/penEasy, but the waist perimeter for Rex and for Regina is calculated measuring the two perpendicular dimensions of their waist and assuming it forms a perfect ellipse (Figure 10): waist (Regina) = 72.36 cm; waist (Rex) = 80.85 cm

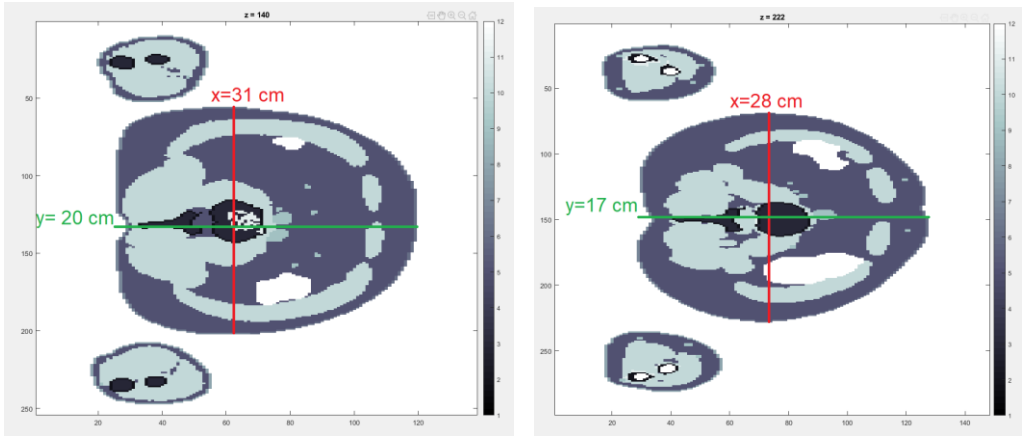

Figure 10: Rex and Regina waist dimensions.

Thus, the scaling values applied to each voxel are:

$$MEN:\ scale_{width} = scale_{depth} = \frac{\left[3.3602 * BMI_{men}\left(\frac{kg}{m^2}\right) + 8.599\right]}{80.85} \quad (7)$$

$$scale_{heigth} = \frac{Height(cm)}{177.60}$$

$$WOMEN:\ scale_{width} = scale_{depth} = \left[3.0254 * BMI_{women}\left(\frac{kg}{m^2}\right) + 11.787\right] / 72.36 \quad (8)$$

$$scale_{heigth} = \frac{Height(cm)}{168.432}$$

II.3.2 Operator positioning

For each irradiation the operator is located in the position obtained from the camera tracking. The location of the main operator is determined at the beginning of each irradiation event and it is kept constant all along the event. A more complex simulation scheme with multiple time steps could be implemented if sufficient computational resources were available.

MCGPU-IR needs 4 points to locate the operator: Head; Left Shoulder; Right Shoulder and Hip (labelled as Spine Base in tracking, see Figure 11.

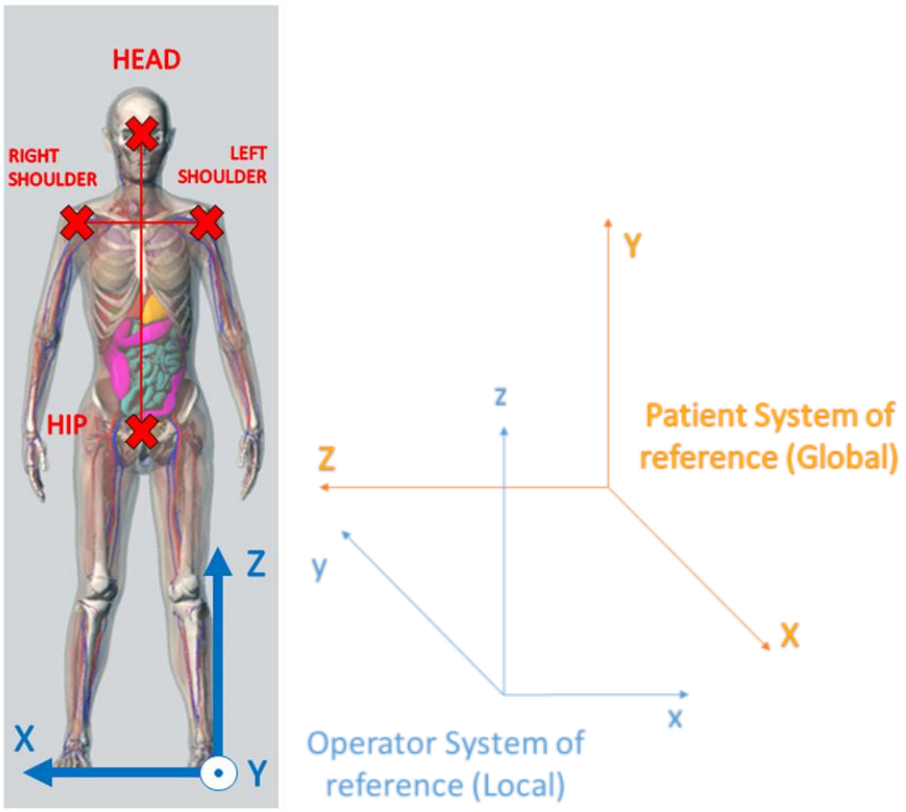

Figure 11: Data for operator positioning (left), patient/operator coordinate systems (right).

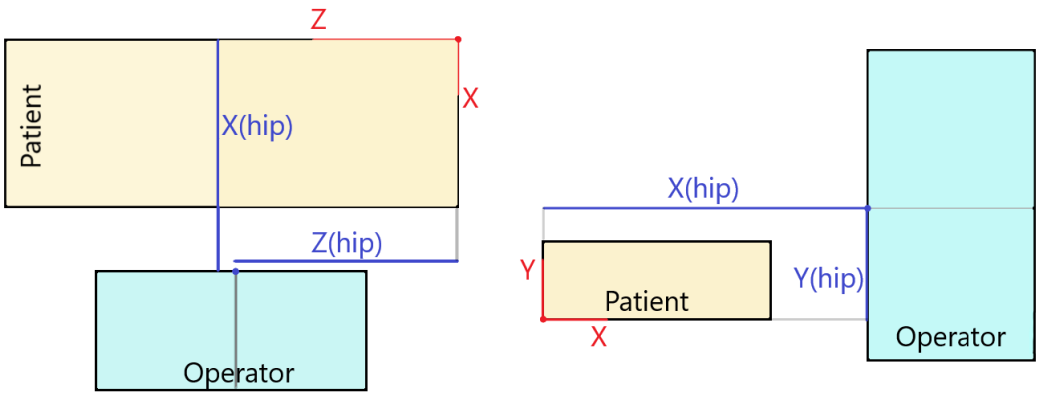

Figure 12: Criteria for positioning the operator using Kinect hip joint location.

The position is calculated from the Hip location as shown in Figure 12. The hip position (x, y, z) determines the distance from the origin of coordinates in MCGPU-IR (left foot of the patient) to the middle point in width and height of the operator.

The other three points needed (shoulders and head) are used for the rotations of the operator phantom, bending over the table and not perpendicular to the table. The rotation of the operator is schematically shown in Figure 13.

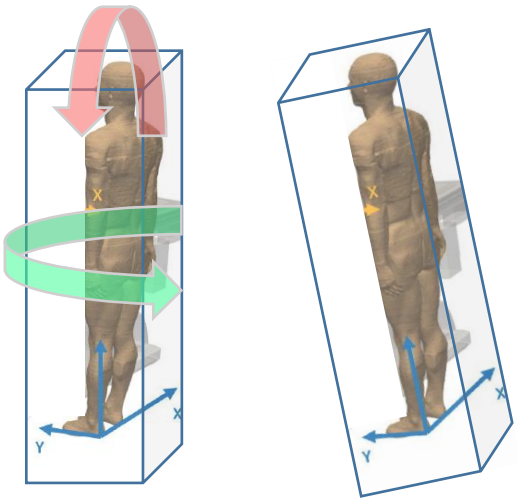

Figure 13: Rotations of the operator.

II.3.3 Normalization to absolute values

For each irradiation event (fixed kV, filtration, angulation and field size values), the air kerma at the reference point (which position is indicated in the RDSR) is calculated by simulating the irradiation of a small box of air centered at the corresponding distance.

II.3.4 II.3.5 Simulation of ceiling-mounted shields

MCGPU-IR allows the user to define a shield interposed between the main operator and the radiation source, however to do it automatically the camera system should provide the position and orientation of the shield. The parameters needed to do it are listed in Table 5. At the present stage of PODIUM project, when shields are present, the geometry files have to be prepared manually.

Table 5. Required information to simulate protective shields.

Value	Description
Rotation angles	Euler angles
Translation	Cartesian coordinates from main operator
Dimensions	Width-Thickness-Height
Attenuation	Attenuation coefficient at mean energy

II.4 Computational resources

PENELOPE/penEasyIR and MCGPU-IR run in the Argos Cluster from INTE-UPC compounded by the following server machines. PENELOPE/penEasyIR uses CPU and it runs in any available node in the cluster. MCGPU-IR instead, uses GPU and it runs only in one node (called c15) with compatible NVIDIA graphic cards.

Cluster head node:

Argos Main Server
DELL Power Edge 420
2 x 1 Intel® Xeon® E5-2470 v2 (2,40GHz, 10N, caché de 25M, QPI de 8,0GT/s, Turbo) 95W, 1600MHz
4 x 16GB RDIMM, 1600MHz
4 x 2 TB SAS nearline 6 Gb/s 7,2K rpm 3,5"
iDRAC Enterprise

Compute nodes:

From c0 to c11:
DELL Power Edge 410
2 x Intel Xeon E5520 Processor (2.26GHz, 8M Cache, 5.86 GT/s QPI, Turbo, HT), 1066MHz Max Memory
8x2GB Dual Rank UDIMMs 1066MHz
1 x 160GB SATA 7200 3,5"
iDRAC Express

c12:
DELL Power Edge 420
2 x 1 Intel® Xeon® E5-2470 v2 (2,40GHz, 10N, caché de 25M, QPI de 8,0GT/s, Turbo) 95W, 1600MHz
4 x 16GB RDIMM, 1600MHz
2 x 2 TB SAS nearline 6 Gb/s 7,2K rpm 3,5"
iDRAC Enterprise

c15:
DELL Power Edge 720
2 x 1 Intel® Xeon® E5-2670 v3 (2,30GHz, 12N, caché de 30M, Turbo) 2133MHz
4 x 16GB RDIMM, 2133MHz
2 x VGAs NVIDIA GeForce 1080Ti 11GB
iDRAC Enterprise

c13 (basic GPU Node):
Intel Core i7 3820 3,60GHz
16 GB RAM DDR3
1 x VGAs NVIDIA GeForce GTX 780 3GB GDDR5
2 x 2TB HD SATA (RAID1)

Argos Xen server (hosting project Virtual Machines):
DELL Power Edge 710
2 x Intel Xeon E5520 Processor (2.26GHz, 8M Cache, 5.86 GT/s QPI, Turbo, HT), 1066MHz Max Memory
8x2GB Dual Rank UDIMMs 1066MHz
3 x 160GB SATA 7200 3,5" (RAID1 + Hot Spare)
iDRAC Enterprise Edition

III. Speed and accuracy tests

III.1 Accuracy tests

As described in D9.110 and D9.113 the accuracy of MC systems has been analyzed in a controlled experimental set-up at Malmö Hospital (Sweden).

Overview of Measurements

Measurements were performed on a static phantom. 2 TLD detectors type TLD 2000C (DC) and 2 Thermo Electron Corp type EPD MK (EMD) for $H_p(10)$ were used for each measurement. The main operator was represented by a CT Torso phantom CTU-41 (Kyoto Kagaku) and the patient phantom was a CIRS Phantom (Adult Male Phantom Model NO. 701). The R100 dose probe (RTI) was used for the measurements in the radiation field.

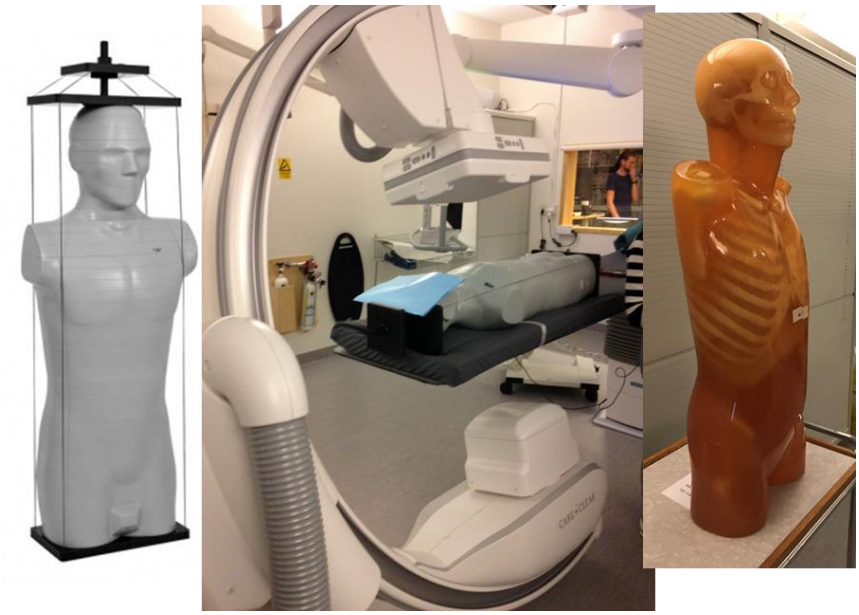

Figure 15: CIRS Rando phantom (left), experimental set-up (center), CT Torso phantom (right).

Exposure field on patient

Two different measurements with the C-arm irradiating the patient on the chest were performed. The first measurements were from 0-degree straight below the phantom and the second measurement was with a 15-degree angle. All machine parameters were taken from the DICOM Radiation Dose Structured Report (RDSR) generated during the exposures. The ceiling mounted lead protection was not used during this case.

The position of the dosemeters for each measurement are given below in Figure 16.

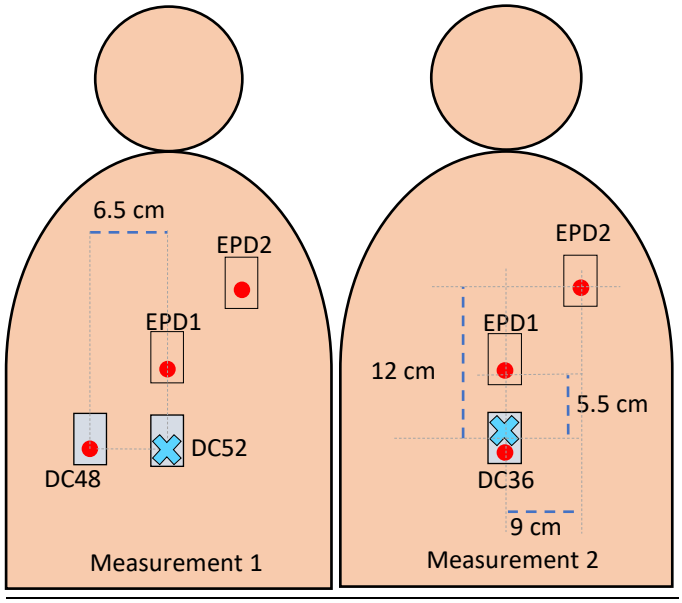

Figure 16: Shows the position of the TLD:s and EPD:s from each separate measurement.

III.1.1 PENELOPE/penEasyIR

With PENELOPE/penEasyIR, patient geometry has been simulated by using different geometries to study the influence of the patient's adapted geometry on the accuracy of the simulated results:

- As a prism (slab) made of soft tissue (ICRU four-component) as described in D9.110.
- As a BOMAB like phantom as described in D9.113, adapted to the real case: chest adapted and without arms and legs. Made of soft tissue.
- As a non-scaled stylized phantom without arms/legs. 4-materials are considered: bone compact (ICRU), soft Tissue (ICRU), skin (ICRP), lung (ICRP). In Figure 17, to show the defined internal organs, soft tissue and skin has been removed for visualization purposes.

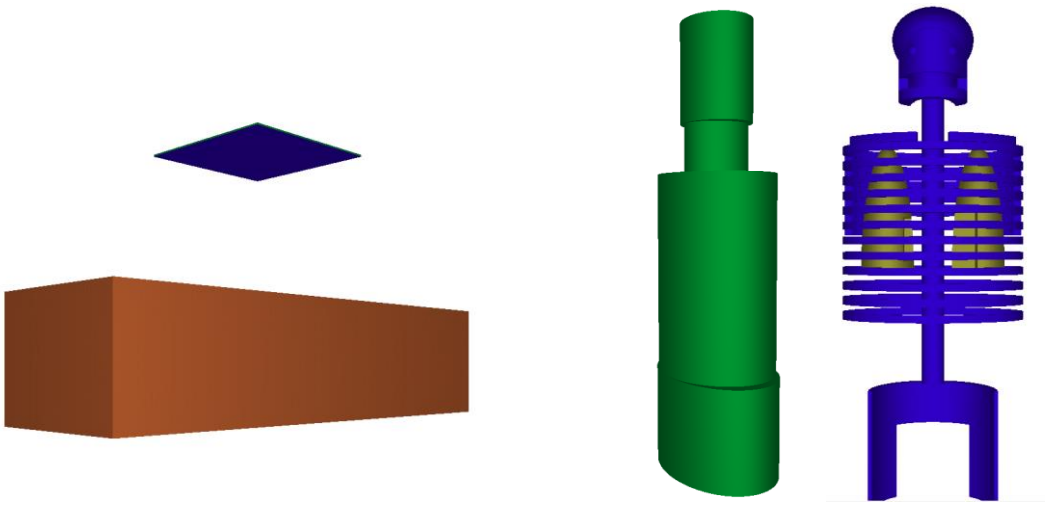

Figure 17: Geometry of prism phantom (left), adapted BOMAB phantom (center), stylized phantom (right).

III.1.2 MCGPU-IR

With MCGPU-IR, patient geometry has been simulated by using different geometries to study the influence of the patient's adapted geometry on the accuracy of the simulated results:

- As a prism (slab) made of soft tissue (ICRU four-component) with the dimensions indicated in Figure 17.
- CT scan of the CIRS Rando phantom, dimensions indicated in Table 6.
- REX scaled phantom (arms and legs included).
- REGINA scaled phantom (arms and legs included).

As mentioned before patient and operator share the same geometry, therefore it means that when, for instance, a CIRS Rando phantom is used to describe the patient, the operator is described by using the same geometry, a CIRS Rando phantom, although the dimensions of the operator and the patient could be scaled separately.

Table 6: Voxel dimensions (Dim) of the CIRS Rando phantom

	Voxels	Dim voxel (cm)	Dim (cm)
X	256	0.15	38.4
Y	256	0.15	38.4
Z	185	0.5	97.5

III.1.3 Analysis of results

Tables 7 and 8 show the simulated $H_p(10)$ compared with the experimental measurements for each detector and each experiment, including the associated uncertainty (k=1). In the case of Monte Carlo data the uncertainty takes into account the statistical uncertainty and an uncertainty of 10 % (k=1) associated to the air kerma value used in the normalization. Simulation times were around 120 s.

Table 7: Experiment 1

	Experimental *Hp*(10)/µSv	**PENELOPE/penEasyIR** $H_p(10)$/µSv			**MCGPU-IR** $H_p(10)$/µSv			
		Prism	**BOMAB**	**Stylized phantom**	**Prism**	**Rando**	**Scaled REX**	**Scaled REGINA**
EPD1	73 ± 8	66 ± 7	84 ± 9	91 ± 9	59 ± 6	80 ± 9	71 ± 7	67 ± 7
EPD2	72 ± 8	56 ± 6	80 ± 8	94 ± 6	50 ± 5	56 ± 6	52 ± 5	48 ± 5
DC52	134 ± 13	84 ± 8	94 ± 9	91 ± 9	56 ± 6	75 ± 8	64 ± 6	57 ± 6
DC48	85 ± 8	63 ± 6	72 ± 7	67 ± 7	75 ± 8	96 ± 10	81 ± 8	75 ± 8

Table 8: Experiment 2

	Experimental *Hp*(10)/µSv	**PENELOPE/penEasyIR** *Hp*(10)/µSv			**MCGPU-IR** *Hp*(10)/µSv			
		Prism	**BOMAB**	**Stylized phantom**	**Prism**	**Rando**	**Scaled REX**	**Scaled REGINA**
EPD1	73 ± 8	51 ± 5	56 ± 6	39±4	47 ± 5	54 ± 6	32 ± 3	54 ± 5
EPD2	63 ± 7	45 ± 4	50 ± 5	42±4	41 ± 4	40 ± 4	28 ± 3	37 ± 4
DC36	103 ± 11	59 ± 6	65 ± 7	39±4	55 ± 6	61 ± 7	34 ± 3	57 ± 6

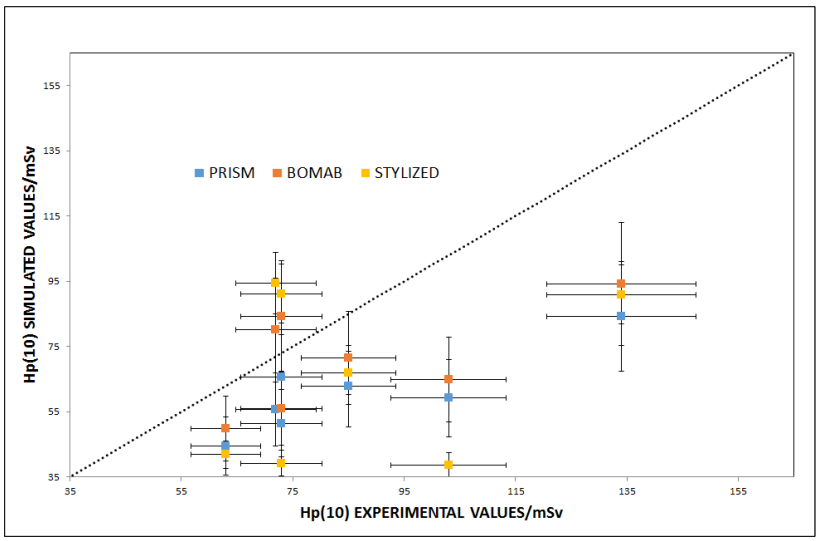

Figure 18: PENELOPE/penEasyIR results using different patient geometries.

As can be observed, for PENELOPE/penEasyIR the geometry description can influence the final result, up to a 30% (experiment 1, EPD2 position) when a prism or the BOMAB phantoms are compared. The use of a stylized phantom can influence the result up to a 40% (experiment 2, DC36 position) when a BOMAB or the stylized phantoms are compared.

As regards MCGPU-IR the geometry description can influence the final result, up to a 35% (experiment 1, EPD1 position) when a prism or the Rando phantom are compared. In addition, when using the REX or REGINA phantoms, the phantom scaling can influence up to a factor of 1.7 (experiment 2).

Taking BOMAB and Rando phantoms data as the best estimates for PENELOPE/penEasyIR and MCGPU-IR respectively, the results are considered satisfactory. The ratio obtained varied between 0.77 and 1.15 for the 4 EPDs measurements for PENELOPE/penEasyIR, 0.63 and 1.10 for MCGPU-IR. As regards the comparison with the 3 TLDs, the ratios are of the same magnitude.

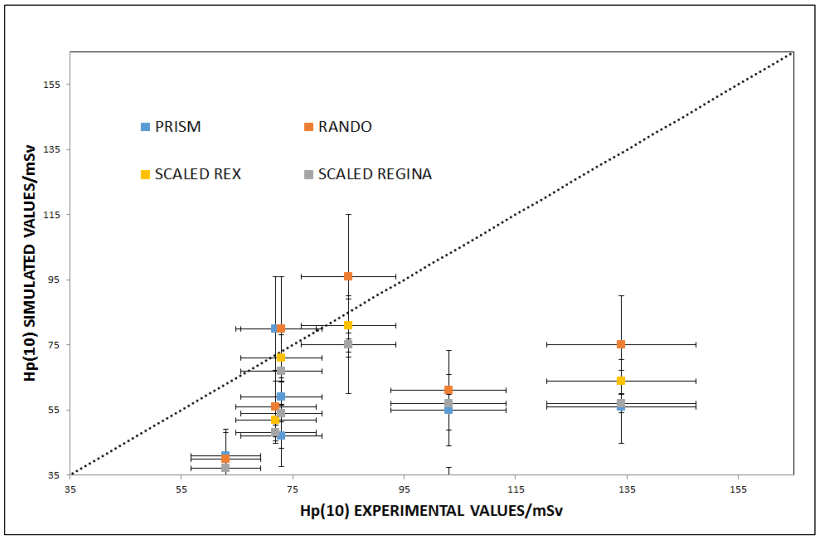

Figure 19: MCGPU-IR results using different patient geometries.

MCCGPU-IR also provided the dose distribution on the worker's body. As can be seen in Figure 20, the dose distribution is quite inhomogeneous, and a slight change in the position to estimate the dose would greatly influence the results. As an illustrative example, the distance between DC48 and DC52 dosemeters is 6.5 cm, and the calculated dose changed a 22 %.

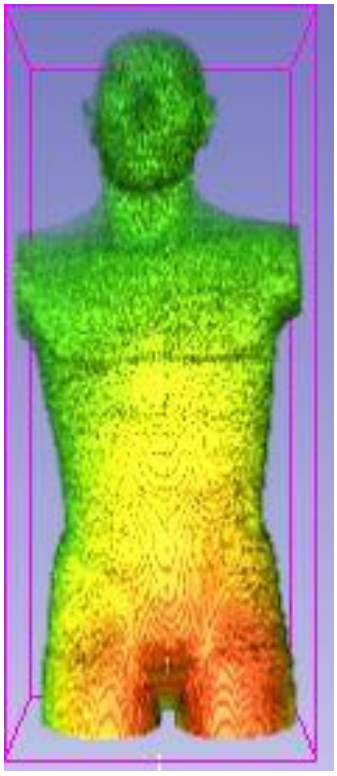

Figure 20: Dose distribution calculated by MCGPU-IR, CIRS Rando phantom.

Finally, to highlight the influence on effective doses of the selection of the voxelized phantom, the effective doses for the scaled REX phantom and the scaled REGINA phantom were computed. Table 9 shows that a difference up to a 30% would be expected by using one or the other.

Table 9: Calculated effective dose for different patient/operator voxel phantoms.

Experiment	*E*/µSv (Scaled REX)	*E*/µSv (Scaled REGINA)
1	28 ± 3	35 ± 3
2	21 ± 2	27 ± 3

III.2 Simulation speed tests

Several speed tests have been carried out to estimate the shortest simulation time that can produce results with a comparable accuracy and acceptable uncertainties. The simulated problem corresponded to the one described in the previous section to assess the accuracy of the codes.

For PENELOPE/penEasyIR, simulation times (use of CPU time) between 2 to 120 seconds have been tested. Figure 21 shows the comparison in terms of statistical uncertainty of the results.

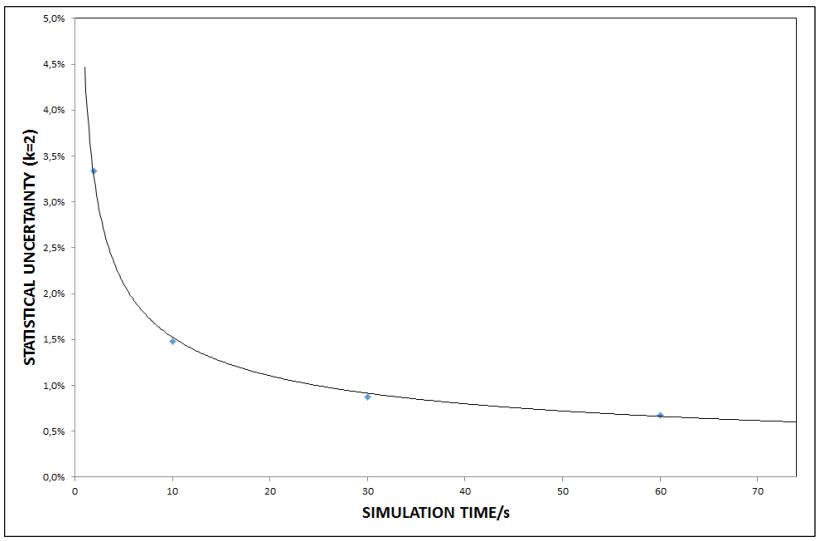

Figure 21: PENELOPE/penEasyIR calculation speed tests.

The absolute values obtained for a simulation time of 2 s agreed with those obtained for 120 s within statistical uncertainties. Therefore it can be concluded that the simulation time can be drastically reduced, however, the global simulation time is also dependent on the time devoted to initialize the code, read input data and write results. For the computer cluster used in the PODIUM project (see section II.4) the initialization time is around 30 s, and thus for this cluster the global simulation times cannot be reduced below this computational limit.

Finally, to point out that even this limit can be easily reduced by using currently available computers, a Macbook Pro 13" from early 2015 (CPU: 2,7 GHz Intel Core i5, RAM: 8 GB 1867 MHz DDR3, SSD disc) has been tested and the corresponding initialization time was reduced to 10 s.

For MCGPU-IR, simulation times (use of GPU time) between 70 to 2 seconds have been tested. Since validation tests were made in terms of *H*p(10), Figure 22 shows the influence of simulation times in terms of statistical uncertainty of *H*p(10) results.

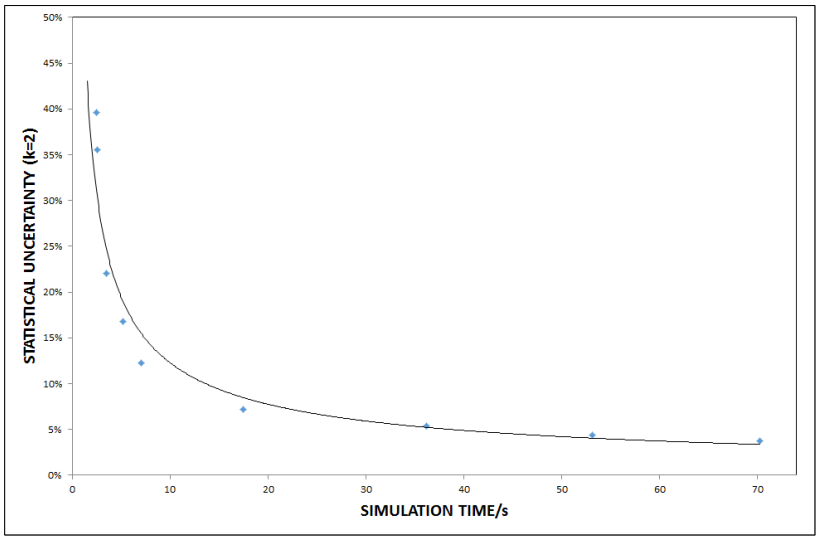

*Figure 22: MCGPU-IR calculation speed tests for H*p(10).

The absolute values obtained for a simulation time of 2 s agreed with those obtained for 120 s within statistical uncertainties. However, it should be reminded that *H*p(10) is calculated by using only a few number of voxels at the detector position. The statistical uncertainty is much lower (< 1% in all cases) for the effective dose since most of sensitive organs are made of thousands of voxels. Figure 23 shows the calculation speed test results for the effective dose calculation.

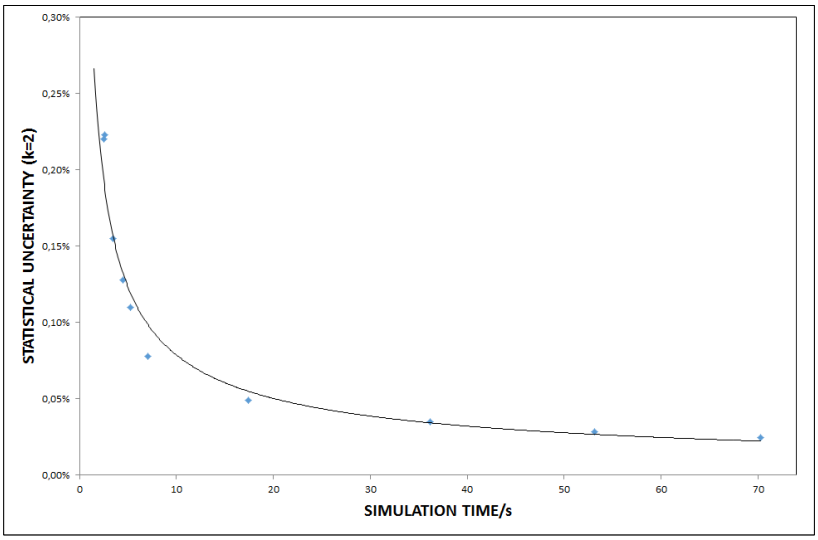

Figure 23: MCGPU-IR calculation speed tests for the effective dose.

As mentioned before, the global simulation time is also dependent on the time devoted to initialize the code, read input data and write output data. For the computer cluster used in the PODIUM project (see section II.4) the initialization time is around 60 s, and thus for this cluster the global simulation times cannot be reduced below this computational limit. However, when a complete realistic procedure has to be calculated, where tens to hundreds of irradiation events should be simulated, MCGPU-IR allows the user to simulate in one single run several irradiation events (up to 30) instead of running a separated simulation for each one. By using this batch technique, the simulation time of 30 events is reduced by a factor 1.3.

To conclude, it is worth mentioning that for PODIUM only 2 GPU cards were available running in our computer cluster, it is foreseen that when using a dedicated GPU cluster with more than two GPUs the computational times would be additionally reduced.

IV. Conclusions

Two fast MC systems have been developed for its application in hospitals for interventional radiology procedures. The two tested codes provided acceptable results in simulation times that can be lower than 20 s (CPU/GPU use time) per simulated irradiation event.

It is worth mentioning that one of the main advantages of MCGPU-IR is the calculation of the effective dose, *E*, but this cannot be verified by comparison with dose measurements because physical detectors can only determine the operational quantities. As shown in Figure 23, the computing time required to calculate *E* is much lower than to calculate $H_p(10)$ with this code. Likewise, when compared to PENELOPE/penEasy, MCGPU-IR offers the advantage to directly calculate *E*. These calculation times for E will of course differ when a lead apron will be present.

V. References

D 9.106 – Guidelines for implementing the workplace geometry and the radiation field map in the dosimetry application. Part 2: Radiation Field Mapping.

D 9.113 - Report from the feasibility study performed in two hospitals.

A.Badal and A. Badano, 2009. Accelerating Monte Carlo simulations of photon transport in a voxelized geometry using a massively parallel Graphics Processing Unit", Medical Physics 36, pp. 4878-4880.

A.Badal, F. Zafara, H. Donga and A. Badano, 2013. A real-time radiation dose monitoring system for patients and staff during interventional fluoroscopy using a GPU-accelerated Monte Carlo simulator and an automatic 3D localization system based on a depth camera. SPIE Medical Imaging conference.

G. Gualdrini et al. 2013. Air kerma to Hp(3) conversion coefficients for photons from 10 keV to 10 MeV for photons from 10 keV to 10 MeV, calculated in a cylindrical phantom. Radiation Protection Dosimetry, 154(4): 517-521 . doi:10.1093/rpd/ncs269.

ICRP, 1996. Conversion Coefficients for use in Radiological Protection against External Radiation. ICRP Publication 74. Ann. ICRP 26 (3-4).

ICRP, 2007. The 2007 Recommendations of the International Commission on Radiological Protection. ICRP Publication 103. Ann. ICRP 37 (2-4).

ICRP, 2009. Adult Reference Computational Phantoms. ICRP Publication 110. Ann. ICRP 39 (2).

ICRP, 2010. Conversion Coefficients for Radiological Protection Quantities for External Radiation Exposures. ICRP Publication 116, Ann. ICRP 40(2-5).

NIST Standard Reference Database 126, last update July 2004 (https://dx.doi.org/10.18434/T4D01F)
ICRP, 1996. Conversion Coefficients for use in Radiological Protection against External Radiation. ICRP Publication 74. Ann. ICRP 26 (3-4).

R. Nowotny and A. Hofer, 1985. XCOMP5, program for calculating diagnostic x-ray spectra. RoeFo, Fortschr. Geb. Roentgenstr. Nuklearmed. 142, 685–689.

J. Punnoose, J. Xu, A. Sisniega, W. Zbijewski, and J. H. Siewerdsena, 2016. Spektr 3.0—A computational tool for x-ray spectrum modeling and analysis. Med Phys. 43(8): 4711–4717.

F. Salvat, 2014. PENELOPE, a code system for Monte Carlo simulation of electron and photon transport.

J. Sempau and A. Badal and L. Brualla, 2011. A PENELOPE-based system for the automated Monte Carlo simulation of clinacs and voxelized geometries. Application to far-from-axis fields. Med. Phys. 38, 5887 – 5895.

Wells JCK, Treleaven P, Cole TJ, 2007. BMI compared with 3-dimensional body shape: the UK National Sizing Survey. Am J Clin Nutr. 85(2):419-25. doi:10.1093/ajcn/85.2.419.